Solar Phys (2008) 249: 53–73
DOI 10.1007/s11207-008-9165-0

Impact Linear Polarization of the Hα Line Observed in a Proton Flare with the Irkutsk Large Solar Vacuum Telescope

N.M. Firstova · V.I. Polyakov · A.V. Firstova

Received: 26 January 2007 / Accepted: 6 March 2008 / Published online: 28 March 2008

Abstract The impulsive phase of the 23 July 2002 2B/X4.8 proton flare with a classical two-ribbon structure was observed with the Irkutsk Large Solar Vacuum Telescope (LSVT) in spectropolarimetric mode, with high spatial, spectral, and time resolution. On the basis of 49 spectrograms and 1200 spectral cuts across the flare ribbons, evidence for Hα line impact polarization has been obtained. A systematic change of the Stokes Q and U parameters has been detected across the ribbons for different flare regions measured with a scanning step of $0.85''$. In the eastern side of the ribbons, the degree of polarization is $4-8\%$; its plane is oriented toward the solar disk center (radial direction). In the western side, the polarization degree runs up to 25%, and its plane is perpendicular to the disk center direction (tangential direction). A comparison of these results with hard X-ray data (RHESSI) allows us to conclude that high-energy electron beams reached the chromosphere during this flare. The observed changes of the direction of polarization and the vanishing polarization within the ribbons mean that, at the chromospheric level, the energy of electrons remaining in the beam is about 200 eV. A shift of the peak position of polarization relative to the intensity maximum in the ribbons may result from the inclination of the electron beam axis with respect to the solar surface.

Keywords Solar flare · Spectrograph · Impact polarization

1. Introduction

The observation of the Hα line impact linear polarization gives unique information on the modes of energy transport from the corona to the chromosphere during solar flares. Hard X-ray and γ-ray observations indirectly prove that chromospheric heating can result from the bombardment of these layers by beams of accelerated particles such as electrons and protons. The relative contribution of protons and electrons to the flare energy budget is not yet

N.M. Firstova (✉) · V.I. Polyakov · A.V. Firstova
Institute of Solar-Terrestrial Physics, Russian Academy of Sciences, Siberian Branch, P.O. Box. 291, Irkutsk 33, 664033, Russia
e-mail: first@iszf.irk.ru

entirely known. Atomic line excitation by collisions with particles having anisotropic distribution functions results in linearly polarized line emission (impact polarization). Therefore, spectropolarimetric observations of the linear polarization of the Balmer Hα line provide one independent diagnostic for energetic particle bombardment of the chromosphere. Such observations have been carried out at the Large Solar Vacuum Telescope (LSVT) of Baikal Astrophysical Observatory. The idea of making diagnostics of the chromospheric heating mechanisms during solar flares by observing impact polarization was first stated by Hénoux and Semel (1981). Since then, some evidence for existence of the impact linear polarization in flares has been obtained (Hénoux *et al.*, 1983a, 1983b, 1990; Hénoux and Chambe, 1990; Hénoux, 1991; Vogt and Hénoux, 1996; Kazantsev *et al.*, 1996; Firstova and Boulatov, 1996; Firstova *et al.*, 1997; Hénoux and Karlicky, 1999, 2003; Firstova and Kashapova, 2001; Firstova, Xu, and Fang, 2003; Xu *et al.*, 2005). However, detailed observation of all the phases of the evolution of a solar flare, with high spatial, spectral, and time resolution, has not been carried out yet. This is due to the difficulties in observing such a rapidly developing phenomenon as a solar flare. Insufficient spatial resolution would make the detection of impact polarization unsuccessful. It seems likely that these very difficulties led to the results presented by Bianda *et al.* (2005), which were based on observations made with low spatial and time resolution and led to the hasty conclusion of the absence of the impact linear polarization in flares.

A 2B/4.8X flare, located at the east limb, was observed with LSVT on 23 July 2002, providing a vast amount of observational material (247 spectrograms) with high spatial, spectral, and time resolution. Only part of this material is considered here. The flare was also observed by RHESSI, TRACE, and other ground-based telescopes. It was widely discussed in the RHESSI special issue (Lin *et al.*, 2003; Holman *et al.*, 2003; Krucker, Hurford, and Lin, 2003), where information on the coronal part of this event is given. Consequently, it is important to study in detail the impact polarization of lines originating in chromospheric layers. Especially because Firstova, Xu, and Fang (2003) presented in the same issue, on the basis of brief analysis, an incorrect conclusion of the absence of polarization in one of the flare ribbons. When analyzing more thoroughly the same spectrograms and other ones, we found that often the polarization, even if actually absent in a ribbon center, is present on both sides of this ribbon.

In Section 2, the procedure used for spectropolarimetric observations of solar flares with LSVT is presented. In Section 3, the flare is briefly described and typical spectrograms are presented. Special attention is given to the orientation of the spectrograph slit during the flare with respect to the direction of the solar disk center. In Sections 4 and 5, the spatial and time distributions of Stokes Q and U parameters are studied. The error estimate on measurements of the polarization is given in the Appendix.

2. Method of Spectropolarimetric Observation

2.1. Spatial and Spectral Resolution of LSVT

The theoretical spatial resolution of LSVT is 0.3 arcsec, but actually this value varies from 0.3 to 1 arcsec depending on atmospheric conditions (Skomorovsky and Firstova, 1996). The slit width when observing flares is 0.35 arcsec. Spectropolarimetric observations are carried out with the CCD camera (TEK 512 × 512, Princeton Instrument). The size of the detector is 0.5×0.5 inch^2; that is, one pixel corresponds to 0.17 arcsec. This value is less than even the theoretical telescope resolution. Because of this, cuts along the dispersion

direction across the slit are usually averaged over three pixels (≈0.5 arcsec), and they are taken every five pixels (0.85 arcsec). Hence, information on a solar surface area of 0.35 arcsec × 0.5 arcsec can be obtained for every 0.85 arcsec. Behind the spectrograph slit there is a Wollaston prism separating ordinary and extraordinary rays that gives a solar spectrum for two orthogonal directions of polarization. Both Stokes Q and U parameters are recorded with the same resolution.

The dispersion of the LSVT spectrograph is high. Because of the finite camera size, we have to observe in the second order of the grating, so about 10 Å can be covered with the CCD. In this process, the spectrograph spectral resolution remains high, $\delta\lambda = 0.023$ Å (with a dispersion of 0.56 Å mm^{-1}).

The spectrograph has a mirror slit. A solar image is obtained from the reflected light by using a birefringent filter with a passband of 0.5 Å in the Hα line.

2.2. Determination of Stokes Q and U Parameters

Polarization observations are carried out with a Wollaston prism, so the ordinary and extraordinary rays propagate in parallel. Since the two spectra in ordinary and extraordinary rays are simultaneously obtained, spurious signals caused by rapid variation of the incident light intensity or by line-of-sight velocities are excluded. When determining the Stokes parameter Q, the radiation polarized along the spectrograph slit is recorded in the upper spectral stripe while in the lower one records the perpendicular polarization (along the dispersion). To obtain the U parameter, a $\lambda/2$ phase plate rotated by 22.5° relative to the slit is set in front of the spectrograph slit. The time interval between the observations of Q and U parameters is usually 6 – 10 s.

Moreover, before the observation began a second $\lambda/2$ phase plate was inserted behind the Wollaston prism to align the oscillation direction of the electric vector of the ordinary and extraordinary beams at 45° with respect to the grooves of the grating. This second $\lambda/2$ plate, in the absence of the first one, was adjusted by equalization of the quiet-Sun intensities in the two spectral bands. It remained fixed during observations.

During daylight hours, the plane of incident and reflected rays rotates by 15° an hour. This leads to a change of the instrumental polarization during observations. The line intensity is normalized to the continuum intensity in each stripe. The instrumental polarization is either totally excluded or brought to a minimum effect, since the Stokes parameter I in the line (without polarization of solar origin) and I in the continuum undergo the same instrumental influence. It has repeatedly been tested that for nonpolarized emission the line profiles in the two spectral stripes are identical. The analysis of the telescope matrix, carried out recently, showed that the intermixing of the Stokes Q/I and U/I parameters results in an absolute error in these parameters of about 1%. The absolute errors in determining the polarization resulting from the instrumental polarization of the telescope and the error in positioning do not exceed 2% (see the Appendix).

In our observations, the Stokes Q/I and U/I parameters were determined by

$$Q/I, U/I = \frac{I_{1\lambda}/I_{1c} - I_{2\lambda}/I_{2c}}{I_{1\lambda}/I_{1c} + I_{2\lambda}/I_{2c}}, \tag{1}$$

where $I_{1\lambda}$ and $I_{2\lambda}$ are the intensities in the line and I_{1c} and I_{2c} are the intensities in the neighboring continuum. The degree of polarization (P) was calculated from the equation

$$P = \sqrt{\frac{Q^2 + U^2}{I^2}}. \tag{2}$$

All data concerning the observation of linear polarization with LSVT are listed in Table 1.

Table 1 Main characteristics of the observational method.

Telescope	LSVT
Detector	CCD – detector TEK 512 ×512
Pixel size	$0.17''$ and 0.01959 Å
Optics of polarization	Rhomboid and two $\lambda/2$ plates
Spectral region	$H\alpha \pm 5$ Å
Spectrograph slit width	70 μm $\approx 0.35''$
Dispersion	0.56 Å mm^{-1}
Exposure time	0.1 s
Sampled area in one spectral cut	$0.35'' \times 0.5''$
Distance between cuts	$0.85''$
Standard errors in Q and U	2%

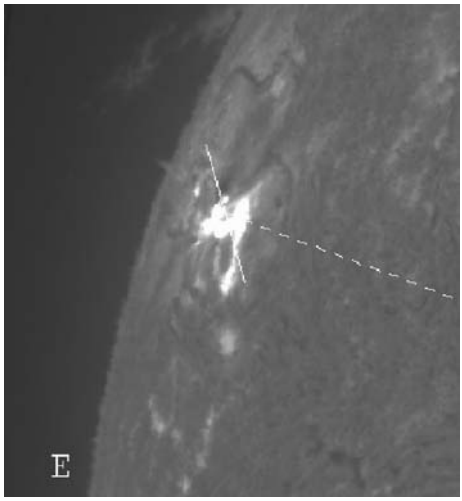

Figure 1 The flare image on 23 July 2002 obtained at Big Bear Solar Observatory. The solid line indicates the position of the spectrograph slit at the beginning of the observation. The dotted line shows the direction to the solar disk center.

3. Observational Data of the 2B/X4.8 Flare

During the observations, the 2B/X4.8 flare was at S13E72 on the solar disk. According to *Solar Geophysical Data* the flare began at 00:15 UT, reached its maximum at 00:35 UT, and ended after 02:00 UT. The LSVT spectropolarimetric observations were made from 00:32:09 UT to 02:55:45 UT. Figure 1 shows a flare image in the Hα line obtained at Big Bear Solar Observatory. The eastern and western ribbons can be seen in this flare region. The solid line shows the position of the LSVT spectrograph entrance slit at the beginning of the observation. The dashed line indicates the direction to the solar disk center, which rotated 15° per hour during the flare.

In Figure 2, the directions of the axis defining the orientation of polarization, with respect to the LSVT spectrograph system and to the solar disk center direction, are shown.

In Figure 2 the ± signs in Q and U mean that, when subtracting the lower spectral stripe from the upper one, the Stokes parameter is, respectively, positive (if $I_1 > I_2$) and negative (if $I_1 < I_2$). The direction to the solar disk center at the first observation moment and the orientation of the polarization plane P obtained in the previous study (Firstova, Xu, and Fang, 2003) are also shown. The direction of the solar disk center rotated by 7.5° and practically coincided with the P direction during the first 30 minutes of the observations.

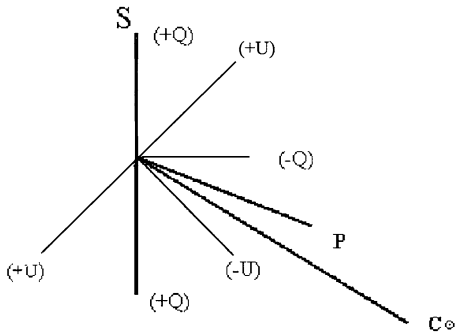

Figure 2 The definition of the polarization plane P in the LSVT spectrograph system with respect to the solar disk center direction. S indicates the orientation of the slit.

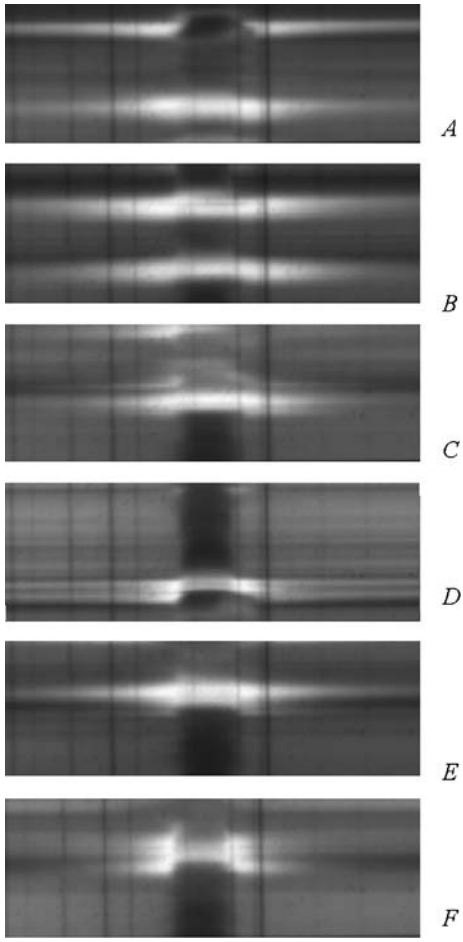

Figure 3 Hα spectrograms obtained in different regions: A region (00:32:09 UT), B region (00:32:48 UT), C region (00:38:58 UT), D region (00:41:17 UT), E region (00:42:11 UT), and F region (00:54:26 UT).

Hence, during the flare observation, the angles between the disk center direction and the $(-Q)$ and $(-U)$ axes are approximately equal. This is also true for the angles between the disk center direction and the $(+Q)$ and $(+U)$ axes. Then, negative values of the Stokes parameters obtained with the LSVT spectrograph system correspond to $P_{||}$ (because they

Table 2 Observational data.

Region	Time interval of observations (UT)	Number of spectrograms	Number of cuts	Number of ribbons
A	00:32:09 – 00:33:59	9	263	2
B	00:32:48 – 00:36:49	14	406	2
C	00:38:52 – 00:39:24	5	114	2
D	00:41:17 – 00:41:42	4	70	1
E	00:42:11 – 00:44:01	8	181	1
F	00:53:20 – 00:54:47	9	166	1

are oriented almost toward the disk center) and positive ones correspond to $P_{\perp}$. The error in the deduced polarization azimuth is estimated to be of the order of $10-15^{\circ}$. It should be kept in mind that theoretically, according to Percival and Seaton (1958), the $P_{||}$ polarization is designated as positive (negative in the LSVT spectrograph system), that is, it results from beam particles of lower energy, whereas $P_{\perp}$ means negative polarization (positive in our system).

Observations by a spectrograph do not permit us to obtain at once a full picture of polarization parameters over the whole flare region. The spectrograph slit was positioned over the most interesting (often merely the brightest) flare regions for which some exposures with the additional $\lambda/2$ plate were made. In this paper, we present six regions with a similar type of spectral behavior. The CCD images of the spectra typical for these six regions are shown in Figure 3.

By now, 49 spectrograms with 1200 cuts (spectral slices) across the slit (along the dispersion) have been processed. In Table 2 are presented the time of observation for each region, the number of spectrograms, and the total number of cuts in each region. The last column is the number of flare ribbons contained in each region. It should be noted that sometimes the flare region observed earlier was rescanned by the spectrograph slit. Therefore in some cases the observing time intervals overlap. The presented data are principally for the impulsive phase of the flare. The data of the main phase of the flare are now being analyzed.

4. Spatial Variations of Stokes Parameters in the Flare

For each spectral cut, the profiles of the line intensity averaged over two stripes $(I_{1\lambda}/I_{1c} + I_{2\lambda}/I_{2c})/2$ and the profiles Q/I or U/I [Equation (1)] were obtained. In the following figures, the spectrograms and the distributions of the profiles I_{λ}/I_{c}, Q/I, and U/I across the flare ribbons are shown.

Figure 4 shows both spectral stripes of the spectrogram, obtained at 00:54:38 UT (region F). The arrows indicate the part of the flare ribbon that we analyzed. In Figure 5, the variations along the slit of the intensity and of the Stokes parameter Q/I are shown. The upper curves correspond to the eastern side of all flare ribbons, and the lower ones to the western side.

Figures 6 and 7 (region B) are similar to Figures 4 and 5 for 00:33:44 UT. The spectrograph slit was positioned across two flare ribbons and the Stokes parameter U was recorded.

In Figure 8, the next two spectrograms obtained for region D at 00:41:17 UT (Q parameter) and 00:41:27 UT (U parameter) are shown. In Figure 9, $(I_1/I_{1c} + I_2/I_{2c})/2$ is presented

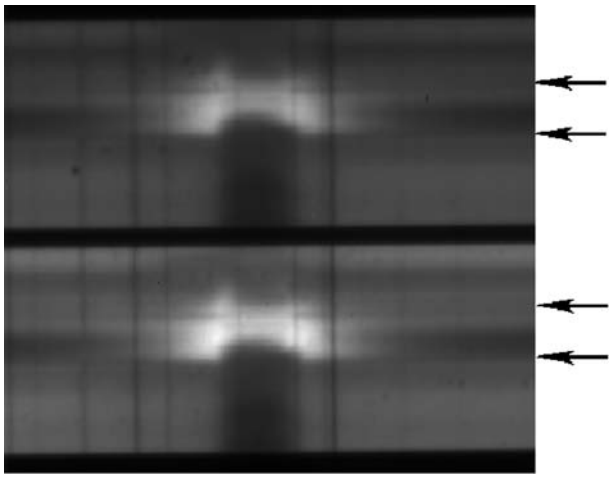

Figure 4 The Hα spectrogram obtained at 00:54:38 UT (region F).

only for 00:41:17 UT (with the intensities being nearly identical in the two spectrograms). The cuts have been made every 3 pixels (0.51″).

All the characteristics, both of the Hα line intensity and of the profiles of Stokes Q and U parameters shown in these figures, are typical of all the observed spectrograms.

Zero values as well as positive and negative values of Stokes Q and U parameters are present in one spectrogram. The maximum values of polarization (up to 20%) have been obtained for those positions along the slit in which the line intensity was not very large.

Vanishingly small polarizations are always seen in the Hα line center no matter whether the Hα line profiles are symmetrical or asymmetrical. The variation of the Stokes polarization profiles along the slit is always considerable (several percent), but there is a certain regularity in this variation.

The majority of the Stokes Q and U profiles both in the presented figures and in other spectrograms are quite narrow. Essentially, their half-widths are 1 – 2 Å; that is, the Stokes Q and U parameters in the line wings (about ± 5 Å) are zero. However, as can be seen in Figure 5, in some cases the Stokes Q parameter is not zero over the entire spectral region. When such a broad polarization component is seen, then, depending on its sign, the Stokes parameter shows either an additional increase or a trough at the line center. Such events were repeatedly observed in the western side of the ribbons, usually only in 2 – 3 cuts with rather low Hα line intensity.

These figures demonstrate the fact that, with considerable averaging over the solar surface (10″ × 10″) done by Bianda *et al.* (2005), the polarization can most probably not be detected. For example in Figure 9, at ≈ 24″ across the ribbon, the Stokes parameters changed signs twice.

The analysis of the polarization for all of the flare regions shows that it does vary across the flare ribbons in the following way: On the eastern side of the ribbons, Q and U are often negative (in our reference system) and usually do not exceed 8%. Their profiles are narrow. As the intensity increases when approaching the center of the ribbons, the polarization becomes close to zero. Sometimes zero values are present only in one cut, and sometimes they can be present in three cuts within the ribbon. When moving into the western side of the ribbon, Q and U increase rapidly to positive values, usually reaching as much as 15% and sometimes 20%. The Stokes Q and U profiles become wide; in this case the change of the profile from narrow to wide is abrupt. This is typical both for single ribbons and for the west one.

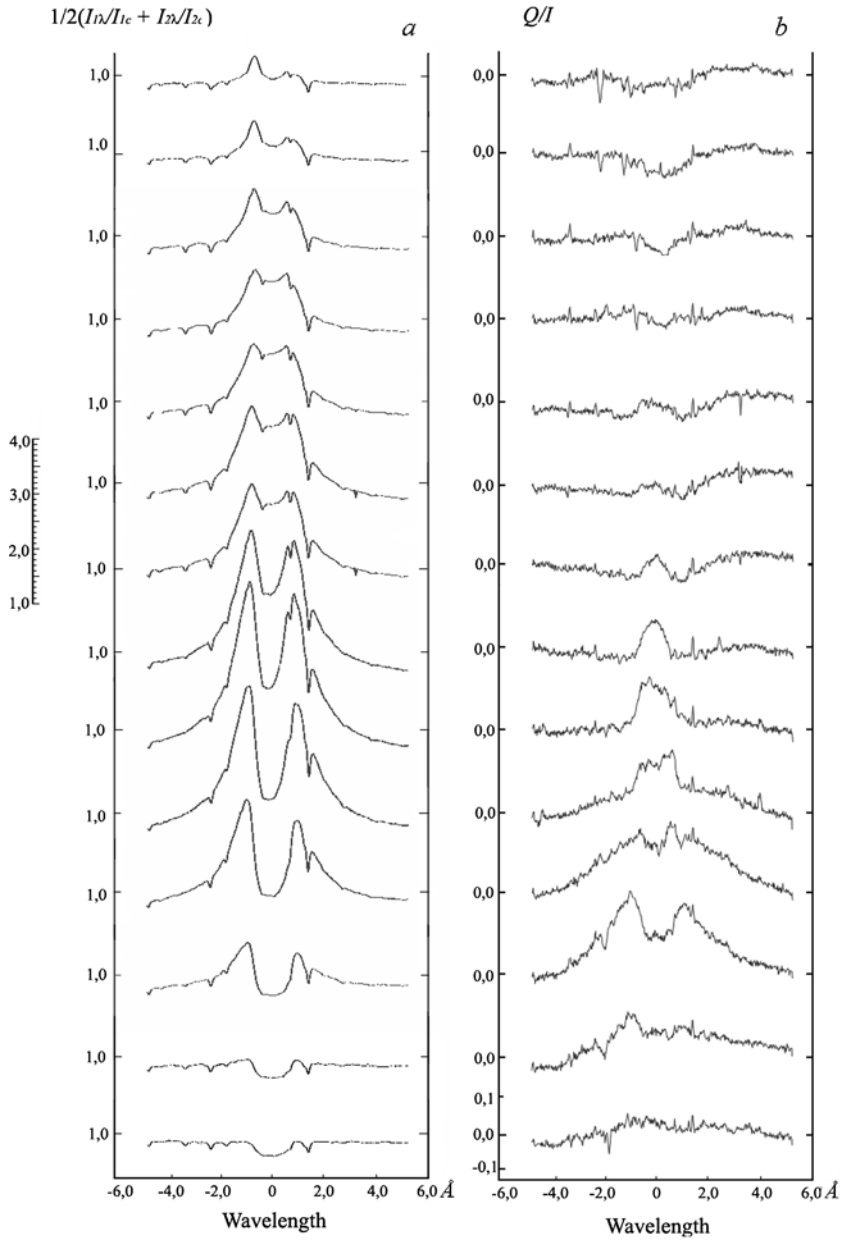

Figure 5 (a) The Hα line profiles at the position along the slit in the spectrogram (00:54:38 UT) for region F; (b) Stokes Q/I profiles at the same position.

5. Spatial and Time Distributions of the Stokes Parameters in Flare Ribbons

The previous section gives examples of the variations of line profiles and Stokes Q and U parameters for some spectrograms. As shown in Table 2, 49 spectrograms for six flare

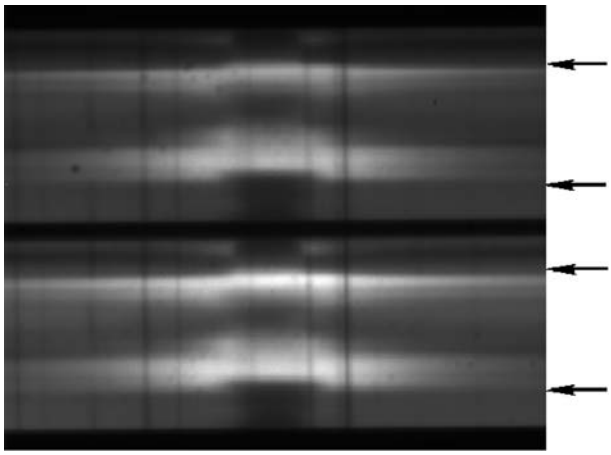

Figure 6 The Hα spectrogram obtained at 00:33:44 UT for region B.

regions were analyzed. Variations in the line intensity and in the Stokes parameters within an individual flare region are insignificant from spectrogram to spectrogram (*i.e.*, in time).

Figure 10 presents the 3D picture of the variations in the line equivalent width $W_i - W_q$ in time (frame number) and along the slit (cut number) for all of the B region spectrograms, where W_i is the line equivalent width of the flare and W_q is that of the quiet Sun (where usually the variations in W_q are $\approx 7-8$ Å). It is evident that over 4 minutes the distribution of the line equivalent width across the flare ribbons has not been changing significantly.

It should be noted that these spectrograms are grouped in series as they have been obtained (*i.e.*, the Q and U parameters alternate). Figure 11 shows separately the spatial distribution of the values of Q and U for the same flare region. It can be noticed that, first, over 4 minutes both parameters vary insignificantly from spectrogram to spectrogram (*i.e.*, in time), while they experience considerable variations from the position along the slit (*i.e.*, in space). Second, the behaviors of the Q and U parameters are similar for this flare region.

In Figure 11, the thick lines represent the distributions of Q and U parameters for three instances: 00:34:39 UT, 00:34:48 UT, and 00:34:55 UT (for U, Q, and U, respectively). Since the time intervals between these spectrograms are short, the polarization degree for 00:34:44 UT and 00:34:51 UT and for all cuts can be calculated by interpolation. For instance, for the 26th cut (at 22.1 arcsec; $Q/I = 0.18$, $U/I = 0.12$, and $U/I = 0.10$) $P \approx 0.21$ for 00:34:44 UT and $P \approx 0.22$ for 00:34:51 UT.

Since the distribution of the Stokes Q and U parameters across the flare ribbons varied only slightly in time, the distribution of the polarization degree was obtained by averaging over observation time. The same averaging was made for the Hα line equivalent width. Figure 12 shows the averaged spatial distributions of the polarization degree P/P_{max} and of the Hα line equivalent width $W_i/W_{i\,max}$ across the ribbons for the B region. Here, $W_{i\,max} = 14.86$ Å and $P_{max} \approx 0.16$ are taken as the units.

As seen from this figure, the highest polarization values are observed in the western sides of both of the ribbons (at positions $6.8-9.35$ and $21.25-22.95$ arcsec). In the central parts of the ribbons, the polarization degree is insignificant.

A similar procedure for determining and averaging the equivalent width and the polarization degree was made for other flare regions as well. In Figure 13, the distributions of $W_i/W_{i\,max}$ and P/P_{max} are shown as a function of position along the slit for A, C, D, E, and F regions. For A, C, D, E, and F regions, the maximum line width $W_{i\,max}$ and polarization

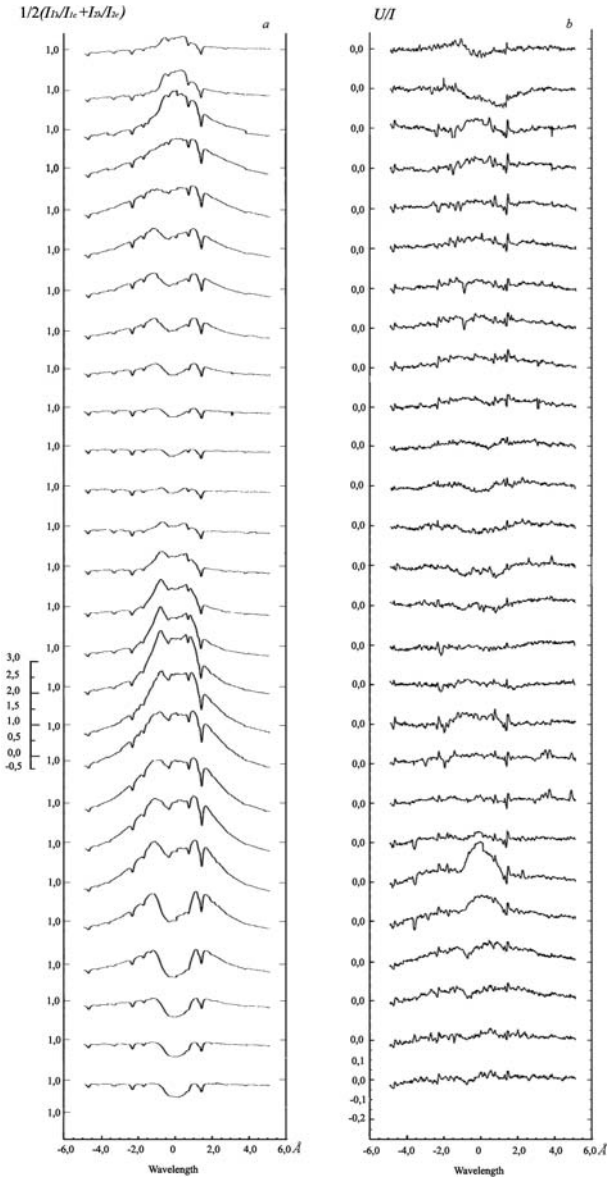

Figure 7 (a) The Hα line profiles at various positions along the slit in the spectrogram (00:33:44 UT) for region B; (b) Stokes U/I profiles at the same positions.

$P_{\max}$ are, respectively, equal to 13.58, 23.8, 11.04, 12.92, and 12.86 Å for $W_{\mathrm{i}\max}$ and 13%, 12.9%, 23.5%, 12.6%, 9.2% for $P_{\max}$.

The distribution of the intensity and polarization degree across the ribbons is practically the same in all regions, including the F region recorded about 20 minutes after the beginning of the observations. A comparison between the distributions of W_{i} and P shows that the peaks of P are in the western side of the ribbons and are shifted to the right (*i.e.*, toward the disk center) of the peaks of equivalent widths in all regions. In the eastern side of the ribbons (to the left in Figure 13), a polarization is sometimes noticeable, especially in A and D regions. The A region, especially in its eastern ribbon, is an exception. Regions A and B

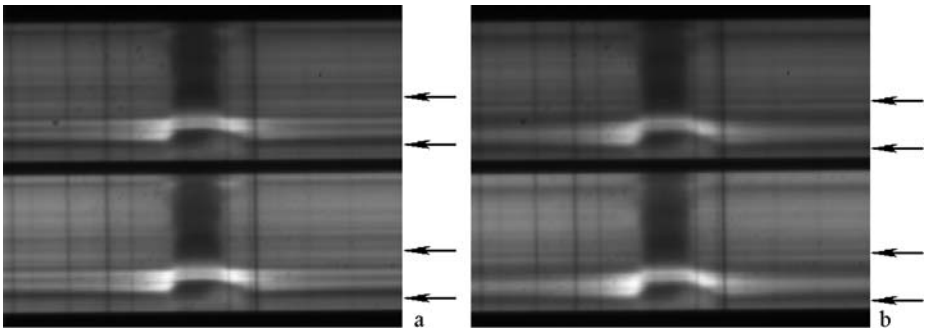

Figure 8 The Hα spectrograms obtained at 00:41:17 UT (Q parameter) and 00:41:27 UT (U parameter) for region D.

were taken at the first 5 minutes after the flare beginning and, in the middle of the eastern ribbon of the A region, there is a considerable central absorption of the line (Figure 3). This central reversal is traced through the line equivalent width (Figure 13), and the negative values of the polarization degree are evident (see the same figure).

We could not integrate the first four spectrograms because of strong time variations of the line intensity, although over 30 s the flare image was unshifted with respect to the spectrograph slit. Therefore we could not determine the polarization degree for these time periods. In the last spectrogram (fourth one), there was no central reversal in the line profile in the eastern ribbon. The line equivalent widths and the Stokes parameter values for these first spectrograms are shown in Figure 14.

In spite of the fact that the distributions of the intensity and polarization across the ribbons differ from spectrogram to spectrogram for the first 30 s of the observation, there are many common features between them as well as with other regions. For the western ribbon, the similarity is clearly identified (*i.e.,* the maximum of the positive polarization takes place when the intensity decreases), whereas in the eastern side of the ribbon the parameter Q is negative. In the eastern ribbon, a rather good agreement with region A is seen at least for the first three spectrograms [*i.e.*, an abrupt change to negative values of parameter Q in the part with a central reversal of the line intensity, and a positive parameter Q at the outer ribbon edges (Figures 14a – 14c)]. The behavior of the intensity and parameter U in the fourth spectrogram (Figure 14d) with no central reversal within the ribbon is similar to their behavior in the B region. However, the ribbons are unusually close to each other.

Regions A – E were observed during the impulsive phase of the flare, whereas the F region was observed during the second X-ray burst. Thus, the flare regions, chosen almost by chance and observed during the first 20 minutes, exhibit a very similar distribution of polarization across the flare.

The distribution of Hα linear polarization in the flare has a small-scale structure. The polarization degree and the shape of the Stokes profiles vary along the slit. These variations take place over a scanning step of 0.85 arcsec. A change in the sign of the Stokes Q and U parameters is repeatedly observed within the flare ribbons. An increase in polarization associated with a decrease in line intensity is often observed, which agrees with other observational results (Xu *et al.*, 2005). According to our previous observations, such a small-scale structure was observed in other flares as well (Firstova and Boulatov, 1996; Firstova, Xu, and Fang, 2003).

Among the analyzed spectrograms, none display a total absence of linear polarization, but all the spectrograms showed some area with zero polarization. Table 3 summarizes the

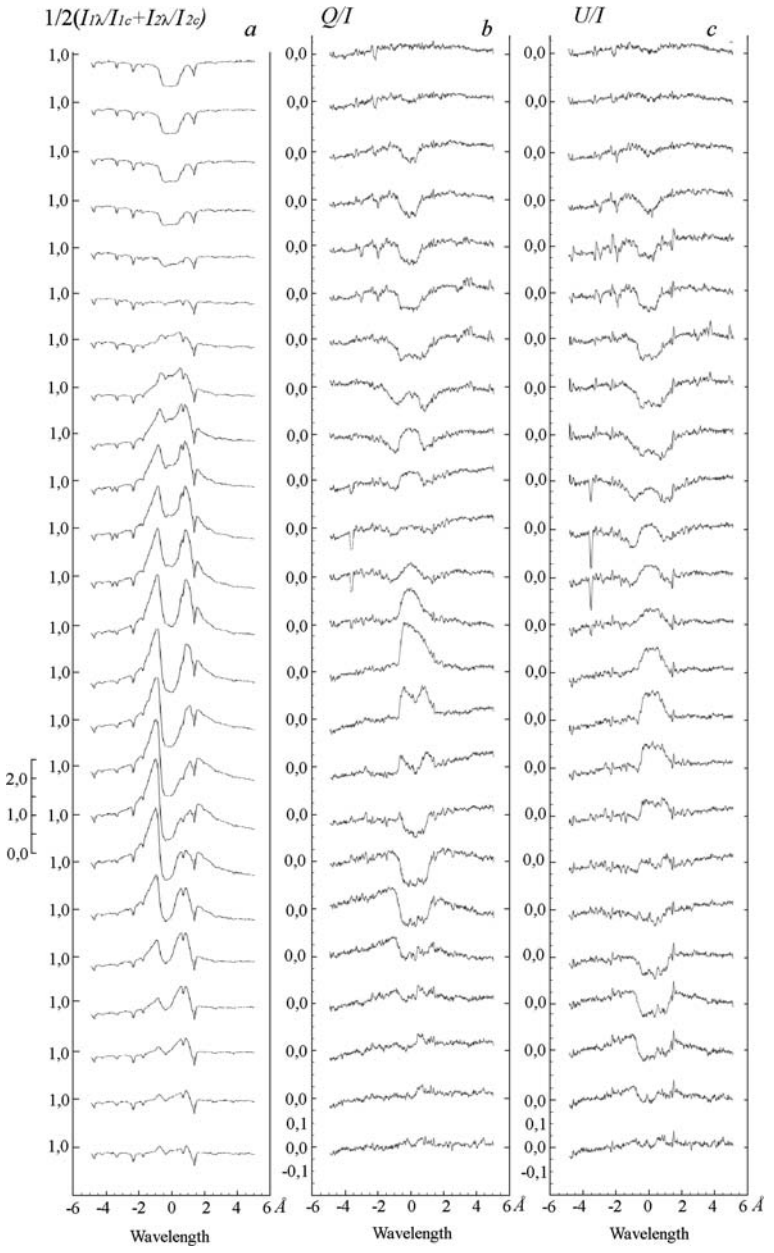

Figure 9 (a) The Hα line profiles at various positions along the slit in the spectrogram (00:41:17 UT) for region D; (b) Stokes Q/I profiles (00:41:17 UT) and (c) U/I profiles (00:41:27 UT) at the same positions.

statistical results of our analysis on the spectrograms that included the six selected regions. In columns 2 – 4, the total number S of the detected polarizations (Q/I_λ and U/I_λ) is given for each region. The $S = 0$ column means the total number of undetected polarizations, but it includes only the measurements in the ribbons. $P_{||}$ corresponds to the polarization in the

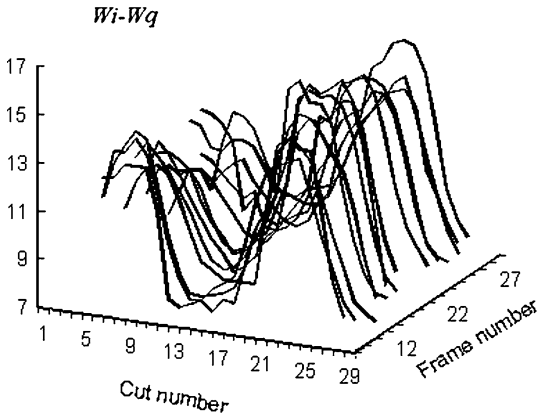

Figure 10 The 3D picture of the line equivalent width as a function of the position along the slit and of the frame number (*i.e.*, time) for all the B region spectrograms.

Table 3 Quantitative characteristic of the observational results.

Region	Number			$P_{\|\|}$ max (%)	$P_{\perp}$ max (%)	I/I_c max
	$S_{\|\|}$	$S_{\perp}$	$S=0$			
A	52	123	88	8.0 ± 0.4	13.0 ± 1.6	2.55
B	32	186	188	1.7 ± 1.4	16.1 ± 3.8	2.95
C	10	58	46	5.8 ± 3.5	12.9 ± 1.7	2.45
D	34	26	10	9.6 ± 3.6	23.5 ± 1.4	2.20
E	19	88	74	2.5 ± 1.7	12.5 ± 1.9	2.85
F	28	76	62	2.6 ± 1.5	13.5 ± 2.1	3.70

direction toward the disk center, and $P_{\perp}$ corresponds to the polarization in the tangential direction.

It is evident from Table 3 that in this flare the polarization orthogonal to the solar disk center dominated.

6. Conclusions

Our analysis of the spectropolarimetric observations of the impulsive phase of the 2B/4.8X proton flare made with the LSVT, with high spatial and spectral resolution, proves the presence of impact linear polarization.

In six regions in the flare, the distribution of Hα linear polarization shows a small-scale structure. Between the spectral cuts separated by 0.85 arcsec, the Stokes parameters Q and U vary. Moreover, a broadening of the Stokes Q and U parameter profiles as well as the occurrence of a central reversal in these profiles has been detected for the first time.

It has been found that the distribution of the degree and orientation of polarization across the flare ribbons is similar for all the observed flare regions. In the eastern side of the ribbon, the polarization degree is 4 – 8%, and the polarization plane is oriented toward the solar disk center (radial direction). In the western side of the ribbon, the polarization plane is perpendicular to the disk center direction (tangential direction) and the polarization degree runs up to 25%. A shift of the peak position of polarization relative to the intensity maximum was regularly observed in all spectrograms.

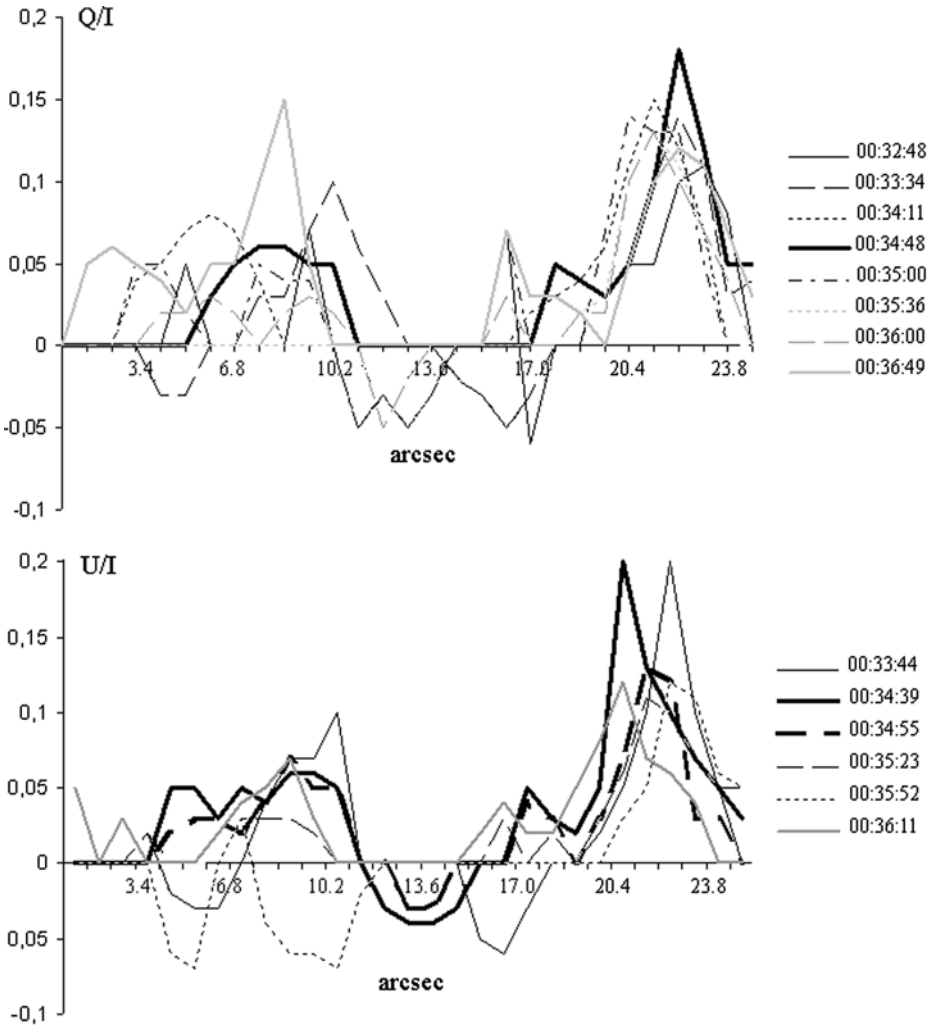

Figure 11 The distribution of Stokes Q and U parameters for all of the B region spectrograms.

The comparison between these results and the hard X-ray (RHESSI) data makes it possible to conclude that the observed Hα linear polarization resulted from the bombardment of the chromosphere by beams of accelerated electrons. The changes of the direction of polarization and the vanishing polarization within the two ribbons imply that the energy of electrons remaining in the beam was about 200 eV at the chromospheric level.

We should look for an explanation of the relative spatial shift between the maximum of polarization and the maximum of intensity in the topology of the magnetic field, namely the direction of the beam with respect to the solar surface. According to Lin *et al.* (2003) and Share *et al.* (2003), the direction of motion of the interacting particles in a magnetic loop is tilted by $\approx 40^\circ$ from the normal to the solar surface toward the Earth. It seems likely that the particles moving along the beam axis with small pitch angles have fallen into the central part of the ribbons. As a result of this process, the dominant emission is generated there in

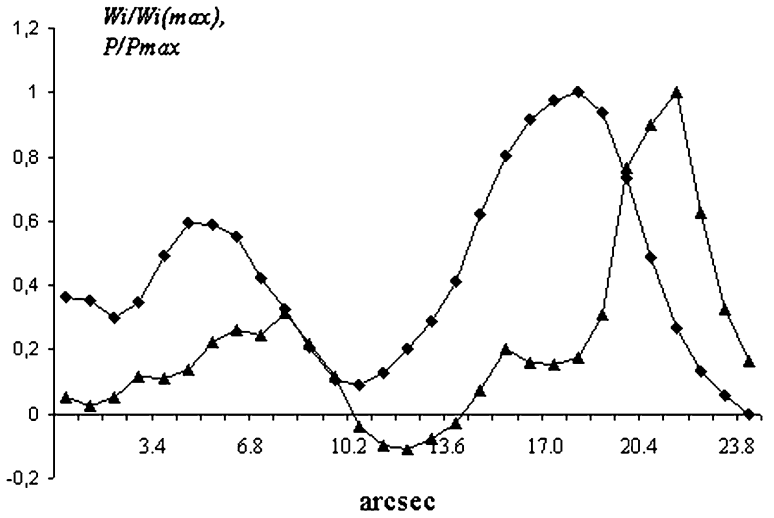

Figure 12 The distributions of W_i (diamonds) and P (triangles) in the B region. These values are normalized to the units of $W_i = 14.86$ Å and $P = 16\%$.

the flare center. At the same time, the angle between the beam axis and the line of sight was only 32°, leading only to a weak or undetectable polarization. However, the beam particles have a certain velocity distribution (Hénoux *et al.*, 1983a, 1983b) and may show a fan-beam structure (Fletcher and Brown, 1995). Therefore, as the high polarization (up to 25%) was observed in the outer western edge of the ribbon, we can assume that there the particles were moving at $\approx 90°$ to the line of sight in this ribbon.

Acknowledgements This study is supported by the Project "Unique Instruments" (No. 02.452.11.7040) and by a supporting grant from Russian leading scientific schools (HIII 4741.2006.2). The authors wish to thank Big Bear Solar Observatory for the Hα solar flare image. The authors also thank the referee for helping to correct the manuscript.

Appendix: Elimination of Instrumental Polarization

The elimination of the instrumental polarization or its minimization was made through the division of the line intensity by the continuum intensity (*i.e.*, by the intensity of initially unpolarized radiation). This radiation was selected at $\approx \pm 5.5$ Å from the line center. We think that at this distance from the line center, for solar disk observations, there is no mechanism resulting in polarization of solar origin. This procedure has been made for every cut in all spectrograms in both spectral stripes. In this way the values $I_{1c} = 1/2[I_{1c}(+5.5) + I_{1c}(-5.5)]$ for the upper spectral stripe and I_{2c} for the lower one were determined.

The degree of linear polarization over the entire line profile was calculated from Equation (1). Such a procedure used in processing the spectrograms leads to a minimization of the instrumental polarization. In the absence of instrumental polarization Equation (1) is correct, as $I_{1c} = I_{2c}$. In the presence of instrumental polarization, the input unpolarized radiation can be written as $\{I_c, 0, 0, 0\}$ and the output one as $\{I_c, X, Y, V\}$, where X, Y, and V

are the polarizations caused by the instrument. The radiation intensities within the two spectral stripes split by the Wollaston prism are

$$\begin{aligned} I_{1c} &= I_c + X, \\ I_{2c} &= I_c - X. \end{aligned} \tag{3}$$

The instrumental polarization degree (since the polarization is absent in the continuum), in terms of the parameter Q/I, is

$$Q/I = \frac{(I_c + X) - (I_c - X)}{(I_c + X) + (I_c - X)}. \tag{4}$$

The Stokes parameters $\{I_\lambda, 0, 0, 0\}$ of unpolarized input radiation become at the exit of the spectrograph $\{I_\lambda, \Delta I_\lambda, Y, V\}$, where ΔI_λ is due to the linear polarization by the telescope ($\Delta I_\lambda = I_\lambda X/I_c$).

Then the intensities of the radiation in the upper and lower stripes in the line are, respectively,

$$\begin{aligned} I_{1\lambda} &= I_\lambda + \Delta I_\lambda = I_\lambda + \frac{X}{I_c}, \\ I_{2\lambda} &= I_\lambda - \frac{X}{I_c}. \end{aligned} \tag{5}$$

Dividing $I_{1\lambda}$ by I_{1c}, and $I_{2\lambda}$ by I_{2c}, and substituting them in Equation (1), one can see that in the absence of solar polarization $Q/I_\lambda = 0$ at all times, independent of the existence of instrumental polarization. Thus, Equation (1) is correct at least in the absence of polarization of solar origin. Let us note that, in all analyzed spectrograms, the polarization often has a significant value in many cuts. We have also obtained zero polarization in several cuts. This means that the absence of linear polarization is equally observed, making us confident about the presence of the linear polarization in the object under investigation. In what follows we consider how adequate our method is to measure linear polarization in a flare.

In the presence of solar polarization, the input radiation $\{I_\lambda, Q, U, V\}$ of a spectral line will become $\{I_\lambda, Q + \Delta I_\lambda + \Delta P_\lambda, U, V\}$ at the output, and the expressions for the line intensity in the upper and lower stripes are

$$\begin{aligned} I_{1\lambda} &= I_\lambda + Q + I_\lambda \frac{X}{I_c} + \Delta P_\lambda, \\ I_{1\lambda} &= I_\lambda - Q - I_\lambda \frac{X}{I_c} - \Delta P_\lambda, \end{aligned} \tag{6}$$

where

$$\Delta P_\lambda = -kQ_\lambda + lU_\lambda. \tag{7}$$

The signs in the Stokes parameters are understandable in such a way that the effect of instrumental polarization on the measured parameter Q tends to decrease Q and to add a false signal caused by U. (For an ideal telescope the matrix should be unitary and diagonal.)

Then, using Equations (1), (2), (6), and (7), we obtain

$$Q/I_\lambda{}^{*M} = \frac{I_c(Q + \Delta P_\lambda)}{I_\lambda I_c - XQ - I_\lambda \frac{X}{I_c} - X\Delta P_\lambda} = \frac{Q/I_\lambda + \Delta P_\lambda/I_\lambda}{1 - X/I_c(Q/I_\lambda - \Delta P_\lambda/I_\lambda - X/I_c)}, \tag{8}$$

where $Q/I_\lambda{}^{*M}$ is the Stokes parameter Q/I_λ obtained with our method.

Table 4 Estimation of the absolute errors in Stokes Q parameters obtained from observations (asterisks) and from our method (*M).

Q/I_λ (%)	U/I_λ (%)	$\Delta P_\lambda/I_\lambda$ (%)	$Q/I_\lambda{}^*$ (%)	$Q/I_\lambda{}^{*M}$ (%)	$\Delta Q/I_\lambda{}^*$ (%)	$\Delta Q/I_\lambda{}^{*M}$ (%)
10	10	−0.0055	15.45	9.48	5.45	0.52
10	20	−0.0015	15.85	9.87	5.85	0.13
20	10	−0.015	24.5	18.66	4.5	1.34

Let us estimate the magnitude of parameters appearing in Equation (8). The investigation of the instrumental polarization of the telescope has been performed more than once by using the rotating polaroid placed in front of the main mirror (Firstova *et al.*, 2006). The diameter of the polaroid (300 mm) is less than that of the lens (760 mm), and in the experiment the outer part of the lens was covered by the diaphragm. Therefore, the telescope matrix obtained from the previous investigations represents only the central part of the beam. Nevertheless, using this matrix we can make a comparative analysis of our method with what is directly obtained in the observed spectrograms. The telescope matrix can be written as

$$\begin{bmatrix} A_{11} & A_{12} & A_{13} & A_{14} \\ A_{21} & A_{22} & A_{23} & A_{24} \\ A_{31} & A_{32} & A_{33} & A_{34} \\ A_{41} & A_{42} & A_{43} & A_{44} \end{bmatrix} = \big[T(-2\beta)\big] \times \begin{bmatrix} 1 & 0 & 0 & \alpha_{14} \\ 0.002 & 0.926 & -0.066 & \alpha_{24} \\ 0.06 & -0.04 & 0.905 & \alpha_{34} \\ 0.056 & 0.061 & 0.097 & \alpha_{44} \end{bmatrix} \times \big[T(2\beta)\big], \tag{9}$$

where $[T(2\beta)]$ is the matrix of rotation.

Then, with the input radiation of the line $\{I_\lambda, Q, U, V\}$ and using a standard formula (without considering I_c), we can write

$$Q/I_\lambda{}^* = \frac{I_{1\lambda} - I_{2\lambda}}{I_{1\lambda} + I_{2\lambda}} = \frac{A_{21}I_\lambda + A_{22}Q + A_{23}U}{A_{11}I_\lambda + A_{12}Q + A_{13}U} = A_{21} + A_{22}\frac{Q}{I_\lambda} + A_{23}\frac{U}{I_\lambda}, \tag{10}$$

as $A_{12} = A_{13} = 0$, $A_{11} = 1$. It is obvious that Equation (10) can be rewritten as follows:

$$Q/I_\lambda{}^* = A_{21} + \frac{Q}{I_\lambda} + \left[-(1 - A_{22})\frac{Q}{I_\lambda} + A_{23}\frac{U}{I_\lambda}\right] = A_{21} + \frac{Q}{I_\lambda} + \Delta P_\lambda/I_\lambda. \tag{11}$$

Let us point out that $X/I_c = A_{21}$ is determined when each spectrogram is processed. By knowing this parameter at the moment of the exposure of a spectrogram, it is possible to determine the 2β angle and consequently other A parameters. On average, during the impulsive phase of this flare, $A_{21} = 0.06$, $A_{22} = 0.905$, and $A_{23} = 0.04$. Hence Equations (8) and (11) include the same parameters and unknowns that permit us to compare these formulas. For some values of Stokes parameters, this comparison is presented in Table 4. There, Q/I_λ and U/I_λ are prescribed values and $\Delta Q/I_\lambda{}^*$ and $\Delta Q/I_\lambda{}^{*M}$ are, respectively, the absolute errors in the Stokes parameters determined without considering the instrumental polarization and using our method.

It is evident from Table 4 that our method essentially eliminates the instrumental polarization effect. At the same time, the analysis of the formulas shows that, even if dividing

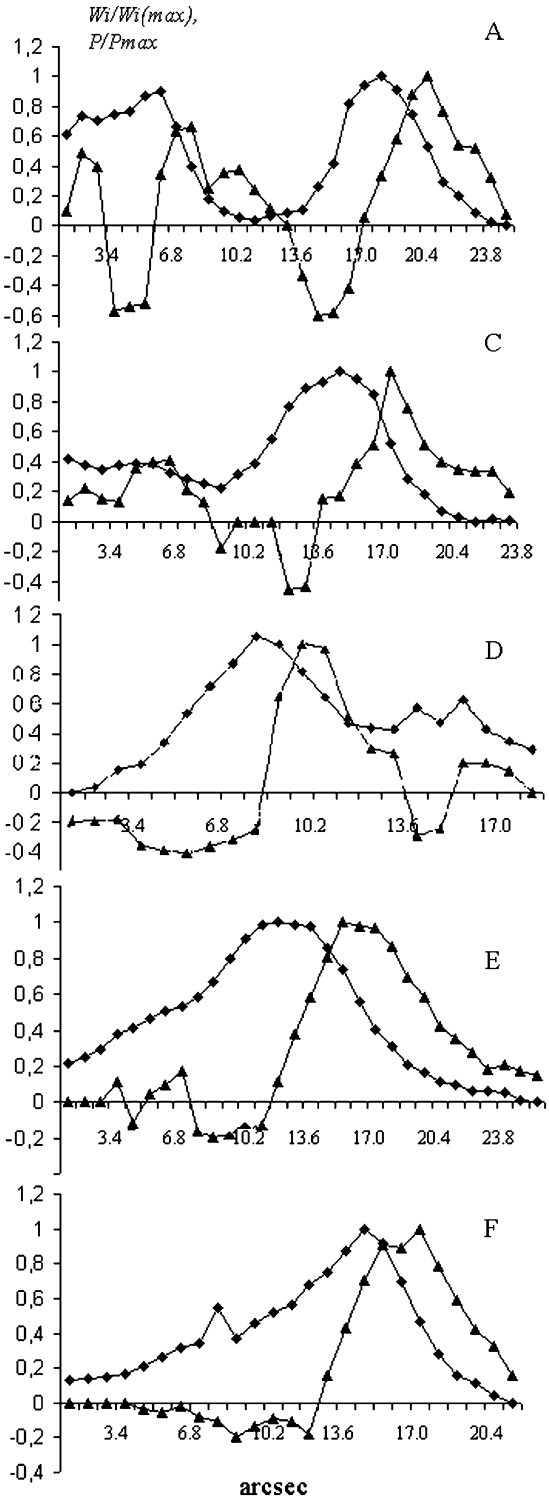

Figure 13 The distributions of W_i (diamonds) and P (triangles) for A, C, D, E, and F regions.

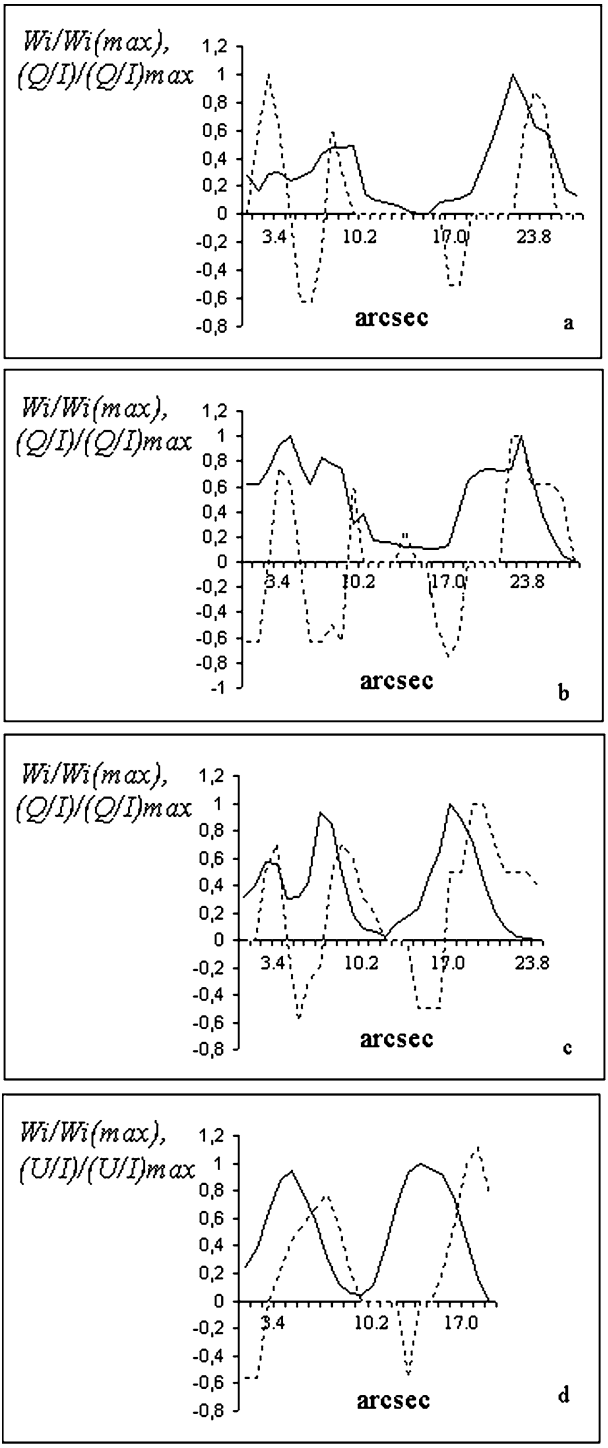

Figure 14 The distributions of the line equivalent width (solid line) and the Stokes Q parameter (dotted line). The values are normalized to the maximum values shown in parentheses for the following spectrograms: 00:32:09 ($W_\mathrm{i} = 11.82$ Å, $Q/I = 8\%$), 00:32:20 ($W_\mathrm{i} = 10.27$ Å, $Q/I = 8\%$), 00:32:27/$I = 10\%$), and 00:32:38 ($W_\mathrm{i} = 14.11$ Å, $U/I = 10\%$).

by the continuum intensity, the contribution from the Stokes I parameter remains more significant than $\Delta P_\lambda / I_\lambda$. This is because I values are an order of magnitude higher than those of Q and U. It may be deduced that even with sufficiently high instrumental polarization the method allows us to determine confidently the linear polarization in solar objects. The absolute errors in the derived Stokes parameters in our method are $\approx 1\%$.

An additional important advantage of this method is that in each spectrogram one can automatically determine the 2β angle to be used in the rotational matrix.

Another possible error may result from possible differences in the location on the solar surface of the regions under investigation by making a pair of cuts in two spectral stripes. As noted already, for each spectrogram in both spectral strips, some cuts across the flare ribbon have been made at $0.85''$ intervals (five pixels). The distance between the upper and lower edges of the stripes determined over all 49 spectrograms is 194.54 ± 0.49 pixels. When processing, the parts of the solar surface in the upper and lower stripes of the spectrum spanning 195 pixels were selected. The error in the identification of these parts is about 0.5 pixel (*i.e.*, $\approx 0.09''$). Let us recall that averaging along the slit was carried out over three pixels, that is, over $0.51''$ of the solar surface. The image resolution, on average, was lower than $0.5''$.

Nevertheless, in the case of a high gradient of the flare intensity along the slit direction, a positioning error of 0.5 pixels can lead to a false polarization signal. To estimate this error, spectral cuts of the line intensity profiles made every five pixels (Figures 5 and 7) and three pixels (Figure 9), averaged over three pixels, were used. The intensity gradient along the slit over a distance of 0.5 pixel was determined by assuming a linear variation of the line intensity over such a small distance.

As a test, this procedure was applied at two points on the Hα line profile: at the line center and in the blue wing. The average value of the false polarization signal was calculated by using 130 points as follows:

$$\frac{Q}{I}\left(\frac{U}{I}\right) = \frac{(I_i + I_{i+1})}{(I_i - I_{i+1})} = 0.094 \pm 0.0012.$$

Thus, the absolute error in the derived Stokes parameters resulting from a misalignment of 0.5 pixels is about 1%.

It seems likely that the absolute error in the derived Stokes parameters from the instrumental polarization of the telescope and from errors in positioning does not exceed 2%.

References

Bianda, M., Benz, A.O., Stenflo, J.O., Kuveler, G., Ramelli, R.: 2005, *Astron. Astrophys.* **434**, 1183.

Firstova, N.M., Boulatov, A.V.: 1996, *Solar Phys.* **16**, 361.

Firstova, N.M., Kashapova, L.K.: 2001, *Issled. Geomagn. Aeron. Fiz. Solnza* **113**, 96 (in Russian).

Firstova, N.M., Xu, Z., Fang, C.: 2003, *Astrophys. J.* **595**, L131.

Firstova, N.M., Hénoux, J.-C., Kazantsev, S.A., Bulatov, A.V.: 1997, *Solar Phys.* **171**, 123.

Firstova, N.M., Polyakov, V.I., Skomopovsky, V.I., Grigoriev, V.M.: 2006, *Soln.-semnayai Fiz.* **9**, 119 (in Russian).

Fletcher, L., Brown, J.C.: 1995, *Astron. Astrophys.* **294**, 260.

Hénoux, J.-C.: 1991, In: *Solar Polarimetry, Proceedings of 11th National Solar Observatory Sac. Peak Summer Workshop*, 285.

Hénoux, J.-C., Chambe, G.: 1990, *J. Quant. Spectrosc. Radiat. Transfer* **44**, 193.

Hénoux, J.-C., Karlicky, M.: 1999, *Astron. Astrophys.* **341**, 896.

Hénoux, J.-C., Karlicky, M.: 2003, *Astron. Astrophys.* **407**, 1103.

Hénoux, J.-C., Semel, M.: 1981, *God Soln. Maksimuma* **1**, 207 (in Russian).

Hénoux, J.-C., Chambe, G., Semel, M., Sahal, S., Wootgate, B., Shine, D., Beckers, J., Machado, M.: 1983a, *Astrophys. J.* **265**, 1066.
Hénoux, J.C., Heristchi, D., Chambe, G., Woodgate, B., Shine, R., Beckers, J., Machado, M.: 1983b, *Astron. Astrophys.* **119**, 233.
Hénoux, J.-C., Chambe, G., Smith, D., Tamres, D., Feautrier, N., Rovira, M., Sahal-Bréchot, S.: 1990, *Astrophys. J. Suppl.* **73**, 303.
Holman, G.D., Sui, L., Schwartz, R.A., Emslie, A.G.: 2003, *Astrophys. J.* **595**, L97.
Kazantsev, S.A., Petrashen, A.G., Firstova, N.M., Hénoux, J.-C.: 1996, *Opt. Spectrosc.* **80**, 709 (in Russian).
Krucker, S., Hurford, G.J., Lin, R.P.: 2003, *Astrophys. J.* **595**, L103.
Lin, R.P., Krucker, S., Hurford, G.J., Smith, D.M., Hudson, H.S., Holman, G.D., *et al.*: 2003, *Astrophys. J.* **595**, L69.
Percival, I.C., Seaton, M.J.: 1958, *Phil. Trans. Roy. Soc. Lond. A* **251**, 113.
Share, R.J., Murphy, R.J., Smith, D.M., Lin, R.P., Dennis, B.R., Schwartz, R.A.: 2003, *Astrophys. J.* **595**, L89.
Skomorovsky, V.I., Firstova, N.M.: 1996, *Solar Phys.* **163**, 209.
Vogt, E., Hénoux, J.-C.: 1996, *Solar Phys.* **164**, 345.
Xu, Z., Hénoux, J.-C., Chambe, G., Karlicky, M., Fang, C.: 2005, *Astrophys. J.* **631**, 618.